Influence of gallium addition on the magnetic properties of MnAl alloy

Thabang Mokwena[1*], *Ramogohlo* Diale[2], *Phuti* Ngoepe[1], and *Hasani* Chauke[1]

[1] Materials Modelling Centre, University of Limpopo, South Africa,
[2]Advanced Materials Division, MINTEK, South Africa

Abstract. The MnAl alloy has the potential to be used in the automotive industry as a permanent magnet due to its good magnetic properties such as high saturation magnetization, large theoretical (BH)max and high Curie temperature. However, this alloy suffers from brittleness and being metastable. In this work, density functional theory (DFT) with a supercell approach was employed to investigate the magnetic and electronic properties of $L1_0$ $Mn_{50}Al_{50-x}Ga_x$ structures. The theoretical lattice parameters are in good agreement with the experimental data, with differences within 2%. Their thermodynamic stability was evaluated from the heats of formation. The heats of formation showed that Ga compromised the thermodynamic stability of MnAl due to an increase in heats of formation. Moreover, the magnetic moment was enhanced as the concentration of Ga increased, indicating that the magnetic strength is enhanced. The Mn 3d contributed more towards the magnetic moment as compared Al and Ga. These findings will positively impact the development of permanent magnets for electric vehicles.

1 Introduction

Permanent magnets (PMs) are essential to the development of modern technologies [1]. Among them, $Nd_2Fe_{14}B$ alloy is preferred because of its superior magnetic properties such as high energy product and remanence. These properties make it suitable for high performance applications. However, $Nd_2Fe_{14}B$ suffers from brittleness and low operating temperatures [2]. It is of significant interest to investigate suitable rare-earth-lean or rare-earth-free permanent magnets to bridge the magnetic performance gap between ferrite magnets and rare-earth-based. Furthermore, the need comes from rare earth elements being expensive and also being harmful to the environment therefore researchers are looking in ways to make permanent magnets that do not contain rare earth elements [3]. Mn-based alloys are promising candidate to replace the rare based magnets. Amongst Mn-based alloys, $L1_0$ MnAl alloy is considered the best candidate due to its excellent magnetic characteristics such as high magnetic moment, high Curie temperature and low density [4]. It has drawbacks, such as being metastable and easily decomposing into β-Mn and Al_8Mn_5 phases at elevated temperatures, and it is also brittle [5, 6, 7, 8]. As a result, the binary Mn-Al alloy's low ferromagnetic τ-phase stability inhibits its application. Using a ternary alloy with different elements (e.g. B, C, or Ga) is one possible way to improve the thermodynamic stability of the τ-phase. It was reported that doping with Carbon in MnAl helps enhance the thermal stability while reducing the internal stress and also contribute to the transformation of $L1_0$-phase into non-magnetic β-Mn and Al_8Mn_5 phases [9].

According to Fang et al. [10], employing drop synthesis techniques, carbon increases the coercivity of MnAl even though the saturation magnetization and Curie temperature are

* Corresponding author: mokwenathabang21@gmail.com

degraded. Ga substitution maintains the magnetic properties of MnAl, presenting a distinct advantage over C doping. Incorporating a small amount of Ga promotes the formation of the thermodynamically stable $L1_0$ phase, which remains unchanged following heat treatment at 700 °C. Despite reports that Ga improves $L1_0$ phase stability without degrading magnetic performance, a systematic DFT investigation of how varying Ga concentrations influence MnAl's magnetic and electronic properties remains limited. [11]. Doping with a relatively small percentage of Tb improved saturation magnetization and coercivity without affecting the formation of $L1_0$ phase during rapid solidification [12]. Wang explored the structural and magnetic properties of MnAl-Zn alloys using the induction melting under argon atmosphere. It was reported that Zn enhances the coercivity and saturation magnetization of the $L1_0$ MnAl, but it compromises the Curie temperature [13]. In this paper, Density functional theory (DFT) was employed to determine the magnetic properties of ternary $Mn_{50}Al_{50-x}Ga_X$ alloys.

2 Methodology

The computational simulations were carried out using the Vienna Ab Initio Simulation Package (VASP) based on DFT [14, 15], where the projector augmented wave (PAW) [16] approach was employed to describe the core-valence electron interactions. The exchange-correlation effects were treated using the generalized gradient approximation (GGA) with the Perdew-Burke-Ernzerhof (PBE) functional [17, 18], while a plane-wave energy cut-off of 500 eV was applied to ensure total energy convergence. According to Monkhorst and Pack, an appropriate k-point mesh of 13x13x10 was employed to converge the structures' overall energy. All calculations were conducted on a 2×2×2 supercell containing 16 atoms, and the VASP substitutional search tool was used to systematically substitute Al with Ga at different atomic percentages. Additionally, elastic constants were determined by applying small strains of 0.005 to all structural configurations.

3 Results and discussion

3.1 Structural and magnetic properties

The equilibrium lattice parameters for different compositions of the $L1_0Mn_{50}Al_{50-x}Ga_x$ alloys are presented in Table 1. The binary model ($Mn_{50}Al_{50}$) was validated by comparing the determined lattice parameters with the theoretical values. For the binary $Mn_{50}Al_{50}$, the calculated lattice parameters are a=2.749 Å (2.750 Å) and c=3.514 Å (3.600 Å) [19] both of which lie below 5% of the theoretical data (the numbers that appear in parenthesis). The presence of Ga reduces a parameter while increasing the c parameter due to its smaller atomic radius compared to Al.

The heats of formation for $L1_0$-$Mn_{50}Al_{50-x}Ga_x$ alloys are displayed in Table 1. The analysis of thermodynamic stability is done using the heats of formation whereby negative heat of formation ($\Delta H_f < 0$) indicates stability, while a positive heat of formation ($\Delta H_f > 0$) indicates instability. The heat of formation is calculated using the formula that follows:

$$\Delta \boldsymbol{H_f} = \boldsymbol{E_C} - \sum_i \boldsymbol{x_i}\, \boldsymbol{E_i}, \tag{1}$$

where E_c is the calculated total energy of the compound, E_i is the calculated total energy of element i in the compound and x_i is the composition of each element. As the concentration of Ga rises, the heats of formation reduce demonstrating that the thermodynamic stability is not improved. Furthermore, the negative heats of formation indicate that these compositions

are thermodynamically feasible for synthesis. Moreover, the doped structure that has the highest is $Mn_{50}Al_{43.75}Ga_{6.25}$ the heat of formation energy of -0.244 eV/atom.

Table 1. The calculated lattice parameters (**Å**) and heats of formation, ΔH_f (eV/atom) of $L1_0$ (P4/mmm) $Mn_{50}Al_{50-x}Ga_X$ alloys.

Structures	a	b	c	ΔH_f
$Mn_{50}Al_{50}$	2.749 (2.750) [18]	2.749 (2.750) [18]	3.494 (3.600) [18]	-0.261
$Mn_{50}Al_{43.75}Ga_{6.25}$	2.748	2.748	3.507	-0.244
$Mn_{50}Al_{37.5}Ga_{12.5}$	2.737	2.737	3.544	-0.227
$Mn_{50}Al_{31.75}Ga_{18.75}$	2.731	2.731	3.572	-0.211
$Mn_{50}Al_{25}Ga_{25}$	2.729	2.729	3.578	-0.196

Figure 1 exhibits the magnetic moments of $L1_0$ $Mn_{50}Al_{50-x}Ga_x$ alloys. Magnetic moments were computed to assess the magnetic strength. The magnetic strength increased with addition of Ga, attributed to rising magnetic moments. As the concentration of Ga increases, the number of unpaired electrons increases as well, causing the magnetic moment to have a minimal increase in the magnetic moment. Demonstrating Ga maintains the magnetic moment of MnAl. With 2.422 Bohr magnetons, $Mn_{50}Al_{25}Ga_{25}$ has the highest magnetic moment.

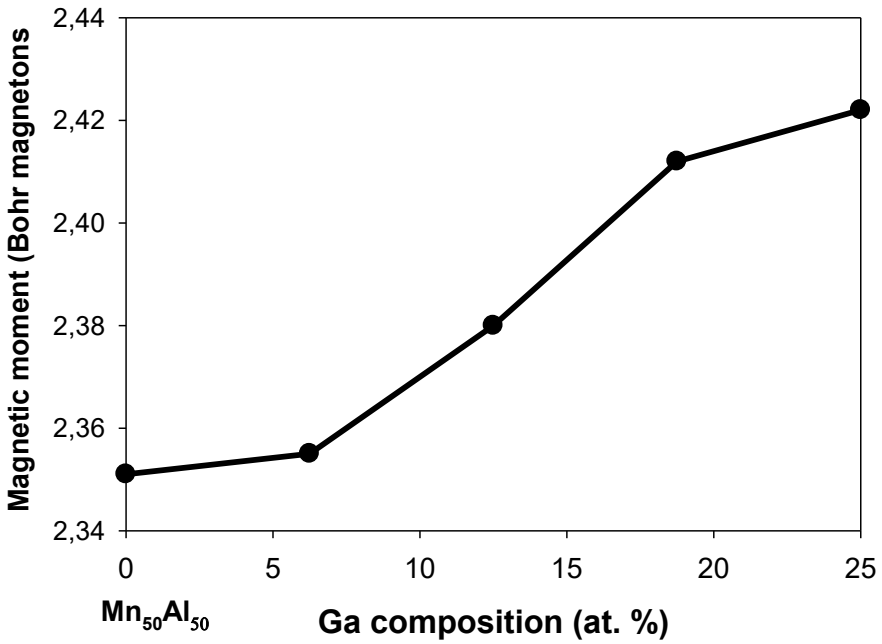

Fig. 1. The total magnetic moment of $Mn_{50}Al_{50-x}Ga_x$ alloys.

The calculated total and partial DOS for $Mn_{50}Al_{50-x}Ga_x$ alloys are shown in Figure 2. To examine the electronic and magnetic characteristics of doped MnAl permanent magnets, the total and partial spin-polarized DOS were computed. These magnetic alloys demonstrated a notable distinction between spin-up and spin-down, which led to net magnetic moments. This DOS analysis confirmed that the $Mn_{50}Al_{50-x}Ga_x$ alloys are ferromagnetic, primarily derived

from the exchange-split Mn-d states. The dominance of Mn-d states near the Fermi level and the evident spin imbalance confirmed that doping with Ga helped MnAl maintain ferromagnetic behaviour. Furthermore, the contribution of Al is from the p orbital compared to s and d orbitals. Additionally, the contribution of Ga is from the p orbital as compared to the s and d orbitals.

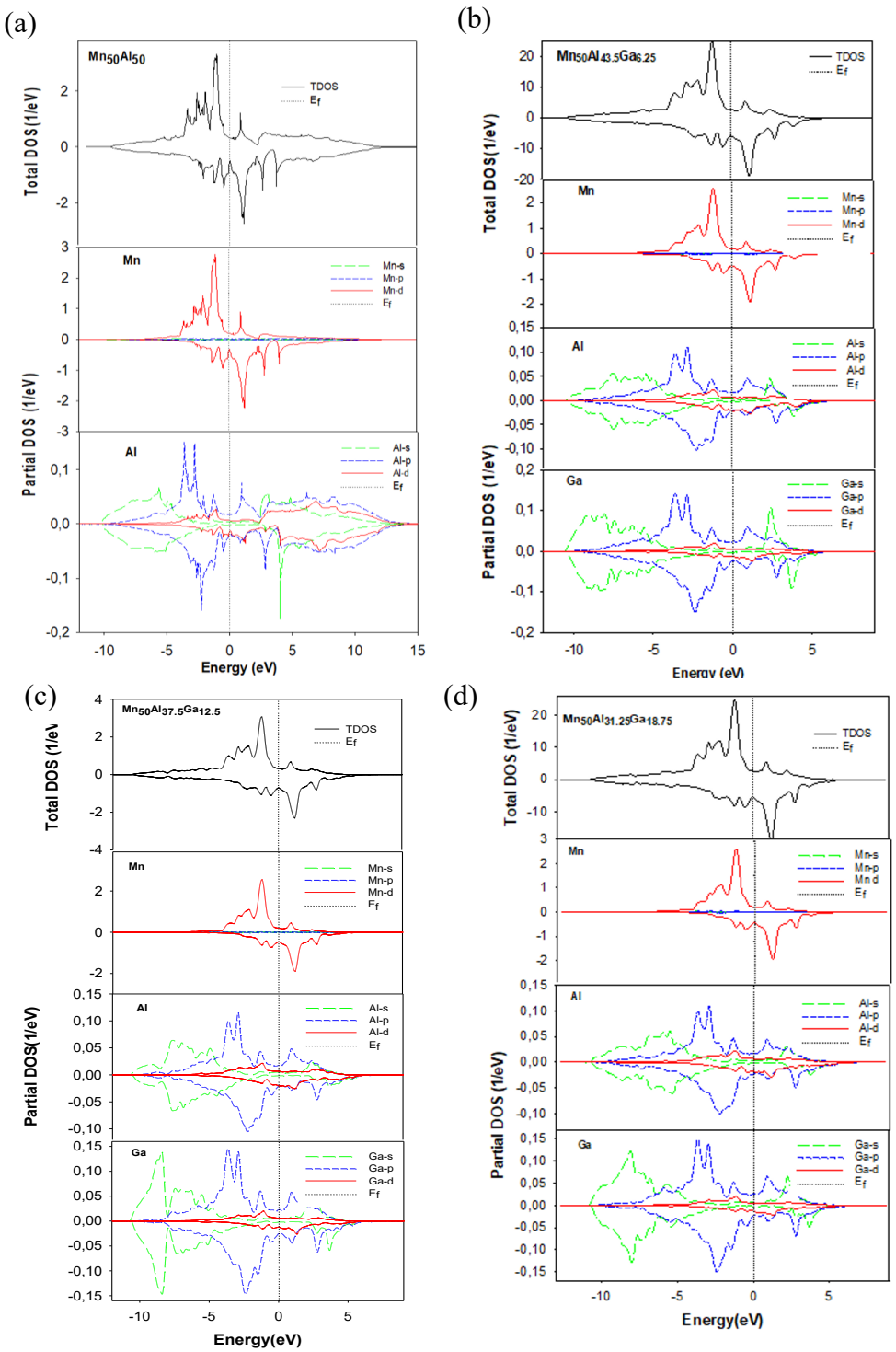

(e)

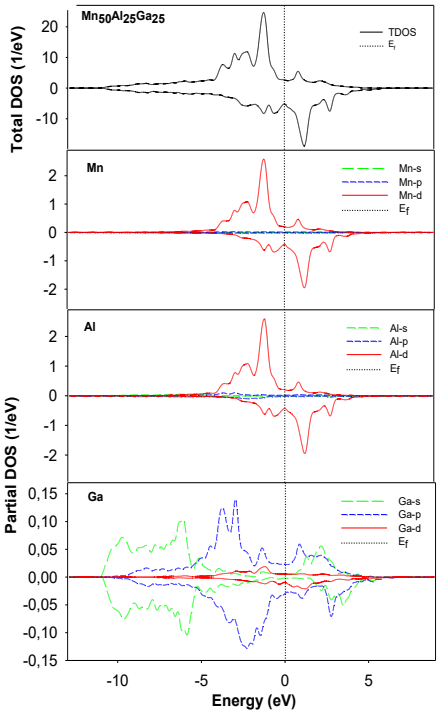

Fig. 2. Total and partial density of states (DOS) for L1₀ $Mn_{50}Al_{50-x}Ga_x$ alloys: (a) x = 0 ($Mn_{50}Al_{50}$), (b) x = 6.25 ($Mn_{50}Al_{43.75}Ga_{6.25}$), (c) x = 12.5 ($Mn_{50}Al_{37.5}Ga_{12.5}$), (d) x = 18.75 ($Mn_{50}Al_{31.25}Ga_{18.75}$), (e) x = 25 ($Mn_{50}Al_{25}Ga_{25}$). The Fermi level is set to 0 eV, indicated by the dashed vertical line.

3.2 Elastic constants and ductility ratios

Evaluating a material's elastic characteristics is necessary since it supports in determining the mechanical stability by utilizing its elastic constants (C_{ij}). They show how crystals react to macroscopic forces, the elastic constants are essential for assessing mechanical strength. Evaluations of multiple systems with various symmetries, such as cubic, tetragonal, orthorhombic, and monoclinic structures, have already been carried out based on the literature. There are six independent elastic constants (C_{11}, C_{12}, C_{13}, C_{33}, C_{44}, and C_{66}.) for tetragonal crystal structures. The mechanical stability condition for tetragonal system is given as follows [20]:

$$C_{44} > 0,\ C_{66} > 0,\ C_{11} > |C_{12}|\ ,\ \text{and}\ \ C_{11} + C_{12} - \frac{2C_{13}^2}{C_{33}} > 0. \quad (2)$$

Figure 3 exhibit the elastic constants of $Mn_{50}Al_{50-x}Ga_x$ structures. All the elastic constants for $Mn_{50}Al_{50-x}Ga_x$ alloys are positive. Additionally for all the compositions the C_{11} is greater than the C_{12} suggesting that all the compositions are mechanical stable. This implies that the crystal structure can withstand small deformations while maintaining its stability, without undergoing spontaneous distortion.

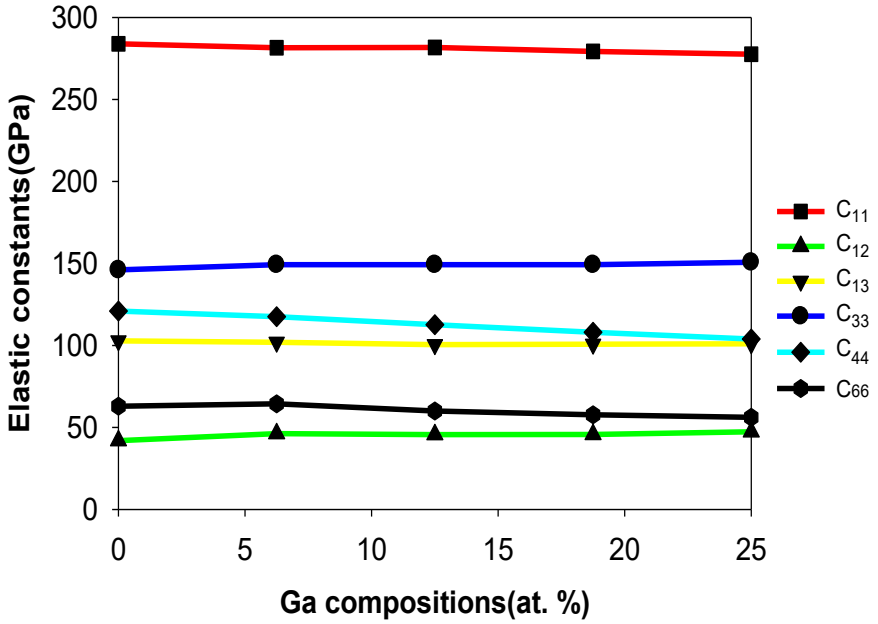

Fig. 3. Elastic constants of $Mn_{50}Al_{50-x}Ga_x$ alloys.

Figure 4 shows the determined Poisson's (σ) and Pugh's (B/G) ratios for the $L1_0Mn_{50}Al_{50-x}Ga_x$ alloys. Pugh proposed using Bulk-to-Shear (B/G) modulus ratios to assess the material's brittleness and ductility. Brittleness is illustrated by a B/G ratio below 1.75, whereas ductility by a ratio above 1.75 [21]. MnAl exhibits brittleness with a computed Pugh ratio of 1.45, consistent with the experimental value of 1.35, and which are less than the critical value of 1.75 [22]. Furthermore, the calculated B/G ratios for all compositions is less than 1.75 suggesting that they are brittle. Addition of Ga improved the B/G ratio.

The ductility of a material was also studied using Poisson's (σ) ratio. A material is considered brittle if the σ is less than 0.26; otherwise ductile [23]. The Poisson's ratio of MnAl is reported as 0.20 in the literature and determined as 0.22 in this study, both below the critical value of 0.26, confirming its brittle nature, with the two values showing good agreement within a 5% difference [22]. The computed Poisson ratio for all compositions were found to be less than the critical value demonstrating that the material is still brittle. Although Ga alloying slightly enhances the elastic properties of MnAl, the persistently high brittleness indices indicate that the material's mechanical performance is still limited under high stress and compression. This suggests that further alloying modifications or alternative processing methods may be necessary to improve ductility. These results are consistent with the calculated B/G ratio results.

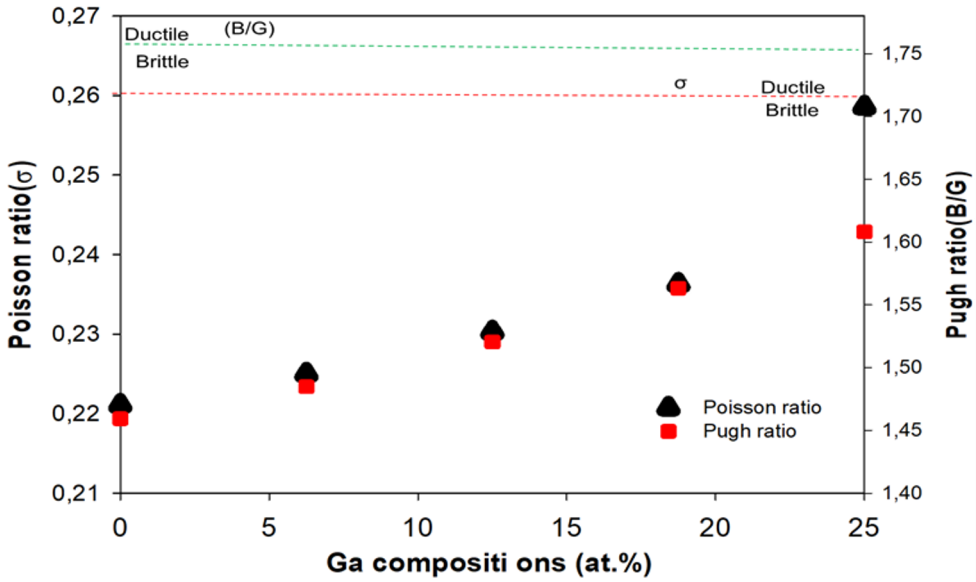

Fig. 4. Pugh and Poisson ratios of $Mn_{50}Al_{50-x}Ga_x$ alloys.

4 Conclusion

The equilibrium lattice parameters, heats of formation, magnetic moments, density of states and elastic properties of $Mn_{50}Al_{50-x}Ga_x$ alloys were investigated using the DFT approach. The results demonstrate that Ga doping enhances the magnetic moment of MnAl which leads to an increase in the magnetic strength, which suggests the potential for high saturation magnetization. As a result of an increase in the heats of formation, Ga destabilizes the MnAl structure. According to the criteria for mechanical stability, all $Mn_{50}Al_{50-x}Ga_x$ alloys are mechanically stable after ternary addition. The Pugh and Poisson's ratios are enhanced with higher Ga concentrations, yet remain below their critical values, indicating that the material retains its brittle character. Consequently, the findings offers insights perspectives on the advancement of the permanent magnet.

The calculations for this study were performed using the facilities of the Materials Modelling Centre at the University of Limpopo and the Centre for High Performance Computing (CHPC) in Cape Town. The authors are grateful for the financial support received from the South African Department of Science and Innovation (DSI) through its Advanced Metals Initiative (AMI) at Mintek and the South African Research Chair Initiative (SARChI).

Open access funding was provided by MINTEK.

Data availability: the findings in this paper is available upon request to the corresponding author.

References

[1] J.M.D. Coey, New permanent magnets; manganese compounds, *J. Phys.: Condens. Matter*, **26**, 064211 (2014).

[2] O. Gutfleisch, M.A. Willard, E. Brück, C.H. Chen, S.G. Sankar, J.P. Liu, Magnetic materials and devices for the 21st century: stronger, lighter, and more energy efficient, *Adv. Mater.*, **23**, 821–842 (2011).

[3] K. Stegen, Heavy rare earths: supply chain challenges and strategic responses, Energy Policy, **79**, 1–8 (2015).

[4] M.J. Kramer, R.W. McCallum, I.A. Anderson, S. Constantinides, Prospects for non-rare earth permanent magnets for traction motors and generators, *JOM*, **64**, 752–763 (2012).

[5] H. Okamoto, T.B. Massalski, The Mn–Al (manganese–aluminum) system, *J. Phase Equilib.*, **15**, 500–521 (1994).

[6] H. Kono, Magnetic properties of manganese–aluminum alloys, *J. Phys. Soc. Jpn.*, **13**, 1444–1451 (1958).

[7] A.J.J. Koch, P. Hokkeling, M.G. van der Steeg, K.J. de Vos, New material for permanent magnets on a base of Mn and Al, *J. Appl. Phys.*, **31**, S75–S77 (1960).

[8] T. Mokwena, R.G. Diale, P.E. Ngoepe, H.R. Chauke, The phase stability of the binary Mn–Al alloys using cluster expansion and first principle calculations, *SAIP Proc.*, **2024**, 135–140 (2024).

[9] J.M. Le Breton, J. Bran, E. Folcke, M. Lucis, R. Lardé, M. Jean, J.E. Shield, Magnetic and structural properties of Mn–Al–C alloys, *J. Alloys Compd.*, **581**, 86–90 (2013).

[10] H. Fang, S. Kontos, J. Ångström, J. Cedervall, P. Svedlindh, K. Gunnarsson, M. Sahlberg, Mn–Al–C permanent magnet materials produced by rapid solidification and spark plasma sintering, *J. Solid State Chem.*, **237**, 300–306 (2016).

[11] T. Mix, F. Bittner, K.H. Müller, L. Schultz, T.G. Woodcock, Magnetic properties of Mn–Al–C permanent magnet alloys prepared by hot deformation, *Acta Mater.*, **128**, 160–165 (2017).

[12] S. Zhao, Y. Wu, J. Wang, Y. Jia, T. Zhang, T. Zhang, C. Jiang, Magnetic properties of Mn–Al–C alloys prepared by melt-spinning, *J. Magn. Magn. Mater.*, **483**, 164–168 (2019).

[13] H.X. Wang, P.Z. Si, W. Jiang, J.G. Lee, C.J. Choi, J.J. Liu, Q. Wu, M. Zhong, H.L. Ge, Magnetic properties of rapidly solidified Mn–Al–C alloys, *Open J. Microphys.*, **1**, 2 (2011).

[14] G. Kresse, J. Hafner, Ab initio molecular dynamics for liquid metals, *Phys. Rev. B*, **47**, 558–561 (1993).

[15] G. Kresse, J. Furthmüller, Efficient iterative schemes for ab initio total-energy calculations using a plane-wave basis set, *Phys. Rev. B*, **54**, 11169–11186 (1996).

[16] P.E. Blöchl, Projector augmented-wave method, *Phys. Rev. B*, **50**, 17953–17979 (1994).

[17] J.P. Perdew, K. Burke, M. Ernzerhof, Generalized gradient approximation made simple, *Phys. Rev. Lett.*, **77**, 3865–3868 (1996).

[18] W. Kohn, L.J. Sham, Self-consistent equations including exchange and correlation effects, *Phys. Rev.*, **140**, A1133–A1138 (1965).

[19] S. Mao, J. Lu, H. Wang, X. Zhao, D. Wei, J. Zhao, Magnetic properties and phase stability of Mn–Al-based permanent magnet materials, *J. Phys. D: Appl. Phys.*, **52**, 405002 (2019).

[20] M.J. Mehl, B.M. Klein, First-principles calculations of elastic properties of transition-metal aluminides, *Intermetallics*, **1**, 1–26 (1994).

[21] S.F. Pugh, Relations between the elastic moduli and the plastic properties of polycrystalline pure metals, *Philos. Mag.*, **45**, 823–843 (1954).

[22] C. Bhandari, G.N. Nope, T. Lograsso, D. Paudyal, Intrinsic magnetic properties and magnetocrystalline anisotropy of Mn–Al alloys from first-principles study, *Phys. Rev. Mater.*, **8**, 034413 (2024).

[23] I.N. Frantsevich, S.A. Voronov, Elastic constants and elastic moduli of metals and nonmetals, *Nauk. Dumka (Kiev)*, 60–80(1983).